

SID



سرویس های ویژه



سرویس ترجمه تخصصی



کارگاه های آموزشی



بلاگ مرکز اطلاعات علمی



عضویت در خبرنامه



فیلم های آموزشی

کارگاه های آموزشی مرکز اطلاعات علمی جهاد دانشگاهی



PROPOSAL

پروپوزال

مركز آموزش
پروپوزال نویسی و پایان نامه نویسی

کارگاه آنلاین
پروپوزال نویسی و پایان نامه نویسی



مركز آموزش
روش تحقیق و مقاله نویسی علوم انسانی

کارگاه آنلاین
روش تحقیق و مقاله نویسی علوم انسانی



ISI
Scopus

مركز آموزش
آشنایی با پایگاه های اطلاعات علمی بین المللی و ترکیه های جستجو

کارگاه آنلاین آشنایی با پایگاه های اطلاعات علمی بین المللی و ترکیه های جستجو



Heat and Mass Transfer in Nanofluid Flow over an Inclined Stretching Sheet with Volume Fraction of Dust and Nanoparticles

N. Sandeep[†] and M. S. Jagadeesh Kumar

Fluid Dynamics Division, Vellore Institute of Technology, Vellore-632014, India

[†]Corresponding Author Email: sandeep@vit.ac.in

(Received July 9, 2015; accepted September 13, 2015)

ABSTRACT

This paper deals with the momentum, heat and mass transfer behaviour of MHD nanofluid flow embedded with conducting dust particles past an inclined permeable stretching sheet in presence of radiation, non-uniform heat source/sink, volume fraction of nano particles, volume fraction of dust particles and chemical reaction. We have considered Cu-water nanofluid embedding with conducting dust particles. The governing partial differential equations of the flow, heat and mass transfer are transformed into nonlinear ordinary differential equations by using similarity transformation and solved numerically using Runge-Kutta based shooting technique. The effects of non-dimensional governing parameters on velocity, temperature and concentration profiles are discussed with the support of graphs. Also, skin friction coefficient, Nusselt and Sherwood numbers are discussed and presented through tables. Under some special conditions present results have good agreement with the existed results. It is observed a raise in the heat transfer rate due to increase in the fluid particle interaction parameter. It is also observed that an increase in chemical reaction parameter enhances the mass transfer rate of the dusty nanofluid.

Keywords: MHD; Dusty fluid; Nanofluid; Chemical Reaction; Volume fraction; Non-uniform heat source/sink.

1. INTRODUCTION

Past few decades researchers have been investigated and being investigating the momentum and heat transfer characteristics of either dusty or nanofluids through different channels. Through this paper we have initiate the analysis of the momentum, heat and mass transfer behavior of a dusty nanofluid over an inclined stretching surface. Dusty nanofluid is a mixture of the nanofluid and the conducting dust particles. Through this initiation we are trying to investigate the metals or metallic oxides (mm. or micro meter sized) which gives good thermal enhancement by embedding into the various nanofluids.

The behaviour of the laminar flow of dusty gases was first studied by Saffman (1962). Choi (1995) was introduced the concept of nanofluid by immersing nano meter sized particles into the base fluid and found the enhanced thermal conductivity in the base fluid. Vajravelu *et al.* (2011) discussed the convective heat transfer in Ag and Cu-water nanofluids past a stretching surface. Heat transfer characteristics of a dusty gas past a semi-infinite inclined plate was studied by Palani and Ganeshan (2007). Dual solution for a mixed convection flow of

a nanofluid over an exponentially stretching/shrinking sheet was illustrated by Subhashini *et al.* (2014). Choudhury and Kumar Das (2014) studied visco-elastic MHD free convective flow through porous media. Debnath and Ghosh (1988) discussed an unsteady MHD dusty fluid flow between two oscillating plates. Convective heat transport in nanofluid was studied by Buongiorno (2005). Ferdows *et al.* (2014) depicts the boundary layer flow of a nanofluid over a permeable unsteady stretching sheet. Mohan Krishna *et al.* (2014) discussed the radiation and magnetic field effects on an unsteady natural convection flow of a nanofluid past an infinite vertical plate in presence of the heat source.

Krishnamurthy *et al.* (2015) discussed the viscous dissipation effects on the MHD flow over an exponentially stretching surface with fluid particle suspension. Makinde and Aziz (2011) have analyzed boundary layer flow of a nanofluid over a stretching sheet with convective boundary conditions. Singh and Singh (1996) discussed MHD flow of a dusty viscoelastic fluid in a porous medium between two inclined parallel plates. Kabir *et al.* (2012) illustrated the heat and mass transfer of an unsteady MHD free convective flow over an inclined porous plate in presence of heat generation.

Krishnamurthy *et al.* (2015) studied the chemical reaction effects and heat transfer on Williamson fluid over a linearly stretching sheet in porous medium. Affify (2009) has presented a similarity solution for MHD free convective flow, heat and mass transfer over a stretching surface by considering suction and injection effects. Elbashareshy (2001) discussed heat transfer over an exponentially stretching continuous surface in presence of suction. Prasad *et al.* (2010) studied MHD flow and heat transfer over a nonlinear stretching sheet by considering variable fluid properties. Ishak *et al.* (2009) analyzed the influence of transpiration on the flow and heat transfer over a moving permeable surface. Makinde (2005) studied the free convection flow and mass transfer past a moving vertical porous plate in presence of thermal radiation. Radiation and inclined magnetic field effects on unsteady MHD convective flow past an impulsively moving vertical plate was discussed by Sandeep and Sugunama (2014). Chamka (1998) analyzed an unsteady MHD flow and heat transfer from a non-isothermal stretching sheet immersed in a porous medium.

Very recently Sheikholeslami *et al.* (2015) discussed thermal radiation influence on MHD nanofluid flow and heat transfer by using a two phase model. Malyand *et al.* (2014) discussed an unsteady stagnation point flow of a nanofluid by considering slip effects. Flow and heat transfer at a stagnation point over an exponentially shrinking vertical sheet in presence of suction was analyzed by Rohni *et al.* (2014). Heat and mass transfer in peristaltic motion of pseudo plastic fluid flow in a curved channel was studied by Hina *et al.* (2015). MHD flow and heat transfer of a dusty fluid over a stretching sheet was presented by Gireesha *et al.* (2012). Saidu *et al.* (2010) analyzed the MHD effects on convective viscous dusty fluid flow by considering volume fraction of dust particles. Ramesh *et al.* (2012) analyzed the heat transfer characteristics of MHD dusty nanofluid flow over an inclined stretching sheet in presence of non-uniform heat source/sink. Heat transfer in Cu-water nanofluid in an enclosure by considering heat sink and discrete heat source was discussed by Hassan (2014). Mansour *et al.* (2008) studied the influence of chemical reaction and thermal stratification on MHD free convective heat and mass transfer over a vertical stretching.

All the references cited above studied either dusty or nanofluid flows through different channels. In this study we investigated the momentum, heat and mass transfer characteristics of MHD dusty nanofluid flow past a permeable inclined stretching sheet in the presence of radiation, non-uniform heat source/sink, volume fraction of nano particles, volume fraction of dust particles and chemical reaction. In this study we considered Cu-water dusty nanofluid. The governing partial differential equations of the flow, heat and mass transfer are transformed in to nonlinear ordinary differential equations by using similarity transformation and solved numerically. The effects of non-dimensional

governing parameters on velocity, temperature and concentration profiles are discussed with the help of graphs. Also, skin friction coefficient, heat and mass transfer rates are discussed and presented through tables.

2. MATHEMATICAL ANALYSIS

Consider a steady two dimensional laminar MHD boundary layer flow of an incompressible viscous nanofluid embedded with conducting dust particles past an inclined vertical stretching sheet with an acute angle γ . If $\gamma = 0$ then there is no inclination in the channel. The X -axis moves along the stretching sheet and y -axis is normal to it. An external transverse magnetic field $B(x)$ is applied to the flow as shown in Fig. 1. Space and temperature dependent internal heat source/sink (non-uniform heat source/sink) along with radiation effect is taken into account. The dust particles are assumed uniform in size. The spherical shaped nano and dust particles are considered. Number density of dust particles is taken as a constant throughout the flow. Volume fractions of the dust and nano particles are taken into account. T_w, C_w and C_∞, T_∞ are the temperature, concentration near and far away from the surface.

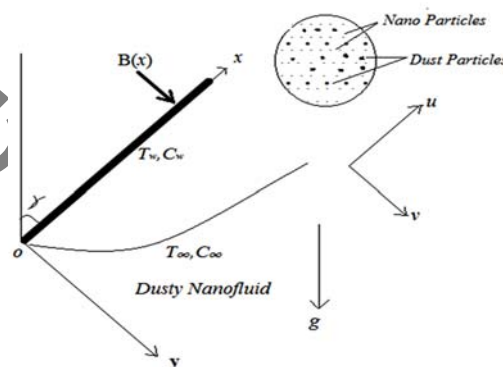


Fig.1. Flow model and physical coordinate system.

Under the above assumptions the boundary layer equations of dusty nanofluid can be written in the form

Flow Analysis:

$$\frac{\partial u}{\partial x} + \frac{\partial v}{\partial y} = 0, \tag{1}$$

$$\rho_{nf} (1 - \phi_d) \left(u \frac{\partial u}{\partial x} + v \frac{\partial u}{\partial y} \right) = KN (u_p - u) + (1 - \phi_d) \mu_{nf} \frac{\partial^2 u}{\partial y^2} + g \left[\frac{(\rho\beta)_{nf} (T - T_\infty)}{+(\rho\beta^*)_{nf} (C - C_\infty)} \right] \cos \gamma + -\sigma B^2 u - \frac{\mu_f}{k_1} u, \tag{2}$$

$$Nm \left(u_p \frac{\partial u_p}{\partial x} + v_p \frac{\partial u_p}{\partial y} \right) = KN (u - u_p), \quad (3)$$

$$Nm \left(u_p \frac{\partial v_p}{\partial x} + v_p \frac{\partial v_p}{\partial y} \right) = KN (v - v_p), \quad (4)$$

$$\frac{\partial(\rho_p u_p)}{\partial x} + \frac{\partial(\rho_p v_p)}{\partial y} = 0, \quad (5)$$

Heat Transfer Analysis:

$$(\rho c_p)_{nf} \left(u \frac{\partial T}{\partial x} + v \frac{\partial T}{\partial y} \right) = k_{nf} \frac{\partial^2 T}{\partial y^2} + \quad (6)$$

$$\frac{N_1(c_p)_f}{\tau_T} (T_p - T) + \frac{N_1}{\tau_v} (u_p - u)^2 - \frac{\partial q_r}{\partial y} + q''' ,$$

$$N_1 C_m \left(u_p \frac{\partial T_p}{\partial x} + v_p \frac{\partial T_p}{\partial y} \right) = -\frac{N_1(c_p)_f}{\tau_T} (T_p - T), \quad (7)$$

Mass Transfer Analysis:

$$u \frac{\partial C}{\partial x} + v \frac{\partial C}{\partial y} = D_m \frac{\partial^2 C}{\partial y^2} - k_o (C - C_\infty), \quad (8)$$

with the boundary conditions

$$\left. \begin{aligned} u = U_w(x), v = 0, T = T_w(x), C = C_w(x) \quad y = 0, \\ u \rightarrow 0, v_p \rightarrow 0, \rho_p \rightarrow \omega \rho, T \rightarrow T_\infty, \\ T_p \rightarrow T_\infty, C \rightarrow C_\infty \quad y \rightarrow \infty, \end{aligned} \right\} \quad (9)$$

The radiative heat flux q_r under Rosseland approximation (Brewster [29]) has the form

$$q_r = -\frac{4\sigma^*}{3k^*} \frac{\partial T^4}{\partial y}, \quad (10)$$

where σ^* is the Stefan-Boltzmann constant and k^* is the mean absorption coefficient. The temperature differences within the flow are assumed to be sufficiently small such that T^4 may be expressed as a linear function of temperature.

Expanding T^4 using Taylor series and neglecting higher order terms yields

$$T^4 \cong 4T_\infty^3 T - 3T_\infty^4, \quad (11)$$

The space and temperature dependent heat generation/absorption (non uniform heat source/sink) q''' is defined as Ramesh *et al.* (2012)

$$q''' = \left(\frac{k_f U_w(x,t)}{xv_f} \right) \left(A^* (T_w - T_\infty) f' + B^* (T - T_\infty) \right), \quad (12)$$

Where A^* and B^* are parameters of the space and temperature dependent internal heat generation/absorption. The positive and negative values of A^* and B^* represents heat generation and absorption respectively. The nanofluid constants are given by

$$\begin{aligned} (\rho\beta)_{nf} &= (1-\phi)(\rho\beta)_f + \phi(\rho\beta)_s, \\ (\rho c_p)_{nf} &= (1-\phi)(\rho c_p)_f + \phi(\rho c_p)_s, \\ \frac{k_{nf}}{k_f} &= \frac{(k_s + 2k_f) - 2\phi(k_f - k_s)}{(k_s + 2k_f) + \phi(k_f - k_s)}, \\ \mu_{nf} &= \frac{\mu_f}{(1-\phi)^{2.5}}, \quad \rho_{nf} = (1-\phi)\rho_f + \phi\rho_s, \end{aligned} \quad (13)$$

where ϕ is the volume fraction of the nano particles. The subscripts f and s refer to fluid and solid properties respectively.

Now, we introduce the following similarity transformations to make the governing Eqs. (1) to (8) subject to the boundary conditions (9) into coupled non linear ordinary differential equations,

$$\begin{aligned} u = \alpha x f'(\eta), v = -\nu_f^{1/2} c^{1/2} f(\eta), \eta = \nu_f^{-1/2} c^{1/2} y, \\ u_p = \alpha x F(\eta), v_p = \nu_f^{1/2} c^{1/2} G(\eta), \rho_p = H(\eta), \\ \theta(\eta) = \frac{T - T_\infty}{T_w - T_\infty}, \theta_p(\eta) = \frac{T_p - T_\infty}{T_w - T_\infty}, \psi(\eta) = \frac{C - C_\infty}{C_w - C_\infty}, \end{aligned} \quad (14)$$

Where $T - T_\infty = A (x/l)^2 \theta(\eta)$, $C - C_\infty = A (x/l)^2 \psi(\eta)$, $l = \nu_f^{1/2} c^{-1/2} > 0$ is a characteristic length, A is a positive constant.

Using the Eqs. (10)-(14), the Eqs. (2)-(8) reduces the following form, Eq. (1) identically satisfies.

$$\begin{aligned} \frac{1}{(1-\phi)^{2.5}} f''' - (1-\phi + \phi(\rho_s / \rho_f)) (f'^2 - ff'') - \\ \frac{(M + K_1)}{(1-\phi_i)} f' + \frac{\alpha\beta}{(1-\phi_i)} H(F - f') + \\ (1-\phi + \phi((\rho\beta)_s / (\rho\beta)_f)) Gr \theta \cos \gamma + \\ (1-\phi + \phi((\rho\beta)_s^* / (\rho\beta)_f^*)) Gc \psi \cos \gamma = 0, \end{aligned} \quad (15)$$

$$GF' + F^2 + \beta(F - f') = 0, \quad (16)$$

$$GG' + \beta(F + G) = 0, \quad (17)$$

$$HF + HG' + GH' = 0, \quad (18)$$

$$\begin{aligned} \left(\frac{k_{nf}}{k_f} + \frac{4}{3} R \right) \theta'' + Pr \alpha \beta_T (\theta_p - \theta) + \\ Pr Ec \alpha \beta (F - f')^2 + (A^* f' + B^* \theta) - \\ Pr \left(1 - \phi + \phi((\rho_p)_s / (\rho_p)_f) \right) (2f' \theta - f \theta') = 0, \end{aligned} \quad (19)$$

$$2F \theta_p + G \theta'_p + \delta \beta_T (\theta_p - \theta) = 0, \quad (20)$$

$$\psi'' - Sc(2f' \psi - f \psi') - Sc Kr \psi = 0, \quad (21)$$

Subject to boundary conditions

$$\left. \begin{aligned} f(\eta) = S, f'(\eta) = 1, \theta(\eta) = 1, \psi(\eta) = 1 \quad \eta = 0, \\ f'(\eta) = 0, F(\eta) = 0, G(\eta) = -f(\eta), H = \alpha \theta(\eta) = 0, \\ \theta_p(\eta) = 0, \psi(\eta) = 0 \quad \eta \rightarrow \infty \end{aligned} \right\} \quad (22)$$

where $\alpha = Nm / \rho_f$ is the mass concentration of the dust particles, $\beta = 1/c\tau_v$ is the fluid particle interaction parameter for the velocity with $\tau_v = m / K$, $M = \sigma B_0^2 / c\rho_f$ is the magnetic field parameter,

$Gr = g\beta_f(T_w - T_\infty) / c^2x$, $Gc = g\beta_f^*(C_w - C_\infty) / c^2x$ are the local Grashof numbers due to the temperature and concentration differences respectively (Kierkus, 1968), $K_1 = v_f / ck_1$ is the porosity parameter, $Pr = v_f / \alpha_f$ is the Prandtl number, $R = 4\sigma^* T_\infty^3 / kk^*$ is the radiation parameter, $\beta_T = 1/c\tau_T$ is the fluid particle interaction parameter for temperature, $Ec = cl^2 / A(c_p)_f$ is the Eckert Number, $\delta = (c_p)_f / c_m$ ratio of the specific heat of the fluid to dust particles, A^* and B^* are the heat source/sink parameters, $Sc = v_f / D_m$ is the Schmidt number and $Kr = k_0A / c$ is the chemical reaction parameter.

For engineering interest the local skin friction coefficient C_f , local Nusselt number Nu_x and local Sherwood number Sh_x are given by

$$C_f Re_x^{1/2} = (1 - \phi)^{-1/2} f''(0), \tag{23}$$

$$Nu_x Re_x^{-1/2} = -(k_{nf} / k_f) \theta'(0), \tag{24}$$

$$Sh_x Re_x^{-1/2} = -\psi'(0), \tag{25}$$

where $Re_x = U_w x / v_f$ is the local Reynolds number.

3. NUMERICAL PROCEDURE

The set of Eqs. (15) to (21) subject to the boundary conditions (22) have been solved numerically using Runge-Kutta based shooting method given by Sandeep and Sulochana (2015). We considered

$$f = f_1, f' = f_2, f'' = f_3, F = f_4, F' = f_5,$$

$$G = f_6, H = f_7, \theta = f_8, \theta' = f_9, \theta_p = f_{10},$$

$$\psi = f_{11}, \psi' = f_{11}$$

Eqs. (15) to (21) are transformed into systems of first order differential equations as follows:

$$f' = f_2$$

$$f_2' = f_3$$

$$f_3' = (1 - \phi)^{2.5} \left[\begin{aligned} & \left((1 - \phi + \phi(\rho_s / \rho_f)) (f_2^2 - f_3) \right) \\ & \frac{(M + K_1)}{(1 - \phi_i)} f_2 + \frac{\alpha\beta}{(1 - \phi_i)} f_7 (f_4 - f_2) + \\ & (1 - \phi + \phi((\rho\beta)_s / (\rho\beta)_f)) G f_8 \cos \gamma + \\ & \left(1 - \phi + \phi((\rho\beta)_s / (\rho\beta)_f) \right) G c f_{11} \cos \gamma \end{aligned} \right] \tag{26}$$

Subject to the following initial conditions

$$\begin{aligned} f_1(0) = f_w, f_2(0) = \lambda, f_3(0) = s_1, \\ f_4(0) = s_2 \dots etc. \end{aligned} \tag{27}$$

In shooting method, we assume the unspecified initial conditions $s_1, s_2 \dots etc$ in Eq. (26), Eq. (27) is then integrated numerically as an initial valued problem to a given terminal point. We can check the accuracy of the assumed missing initial condition, by comparing the calculated value of the different variable at the terminal point with the given value by the existence of the difference in improved values so that the missing initial conditions must be obtained. The calculations are carried out by using the MATLAB programming.

4. RESULTS AND DISCUSSION

The coupled ordinary differential Eqs. (15) to (21) subject to the boundary conditions (22) are solved numerically using Runge-Kutta based shooting technique. The results obtained shows the influence of the non-dimensional governing parameters namely volume fraction of nano particles ϕ , mass concentration of the dust particles α , fluid particle interaction parameter for velocity β , non-uniform

heat source/sink parameter A^* and chemical reaction parameter Kr on velocity, temperature and concentration profiles for fluid and dust phases. For numerical results we considered

$$\delta = 2, M = R = 1, A^* = B^* = \phi = \phi_i = Ec = 0.1,$$

$$\alpha = 0.8, \beta = 0.4, Pr = 6.2, \gamma = \pi / 3,$$

$$Sc = 0.6, \beta_T = Kr = 0.2, Gr = Gc = K_1 = 0.5.$$

These values are kept as common in entire study except the varied values as shown in respective figures and tables. Table 1 shows the thermo-physical properties of water and Copper.

Table 1 Thermophysical properties of water and Cu nano particles.

	ρ (Kgm^{-3})	c_p ($KJg^{-1}K^{-1}$)	k ($Wm^{-1}K^{-1}$)	β ($10^{-5}K^{-1}$)
H_2O	997.1	4179	0.613	21
Cu	8933	385	401	1.67

Figs. 2-4 depict the influence of the nano particle volume fraction on the velocity, temperature and concentration profiles of the flow. It is evident that an increase in the volume fraction of nano particles enhances the velocity, temperature profiles of the fluid and dust phases and depreciates the concentration profiles of the flow. This is due to the fact that an increase in the volume fraction of nano particles enhances the velocity and thermal boundary layer thickness. This enhancement in thermal boundary layer thickness causes to move the particles away from the surface (i.e particles phase moves to cooler areas). Due to this reason we noticed fall in the concentration profiles of the flow.

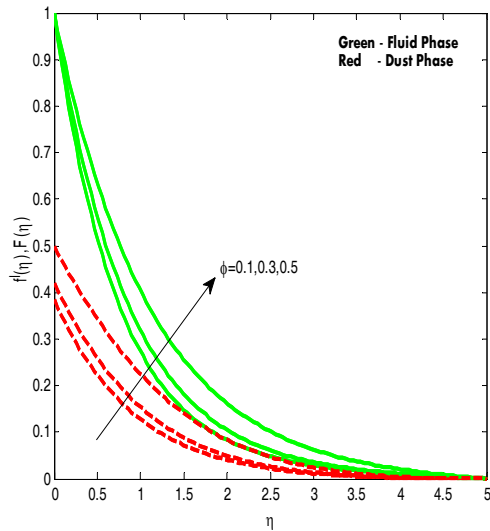


Fig. 2. Velocity profiles for various values of volume fraction of nano particles.

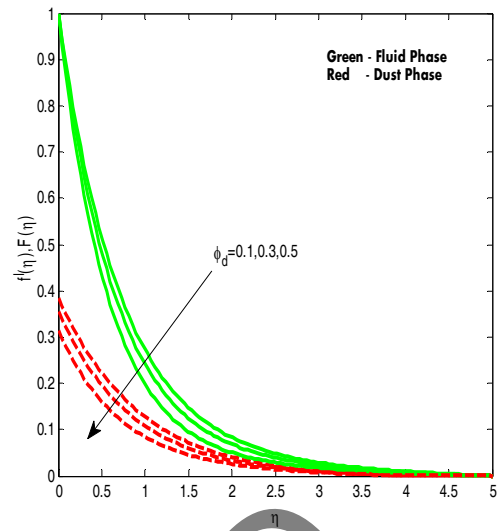


Fig. 5. Velocity profiles for various values of volume fraction of dust particles.

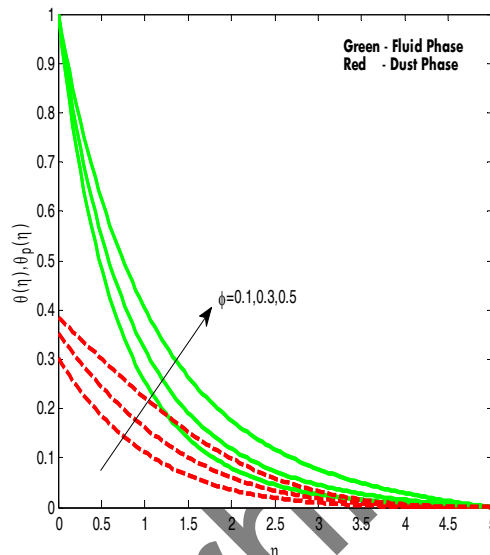


Fig. 3. Temperature profiles for various values of volume fraction of nano particles.

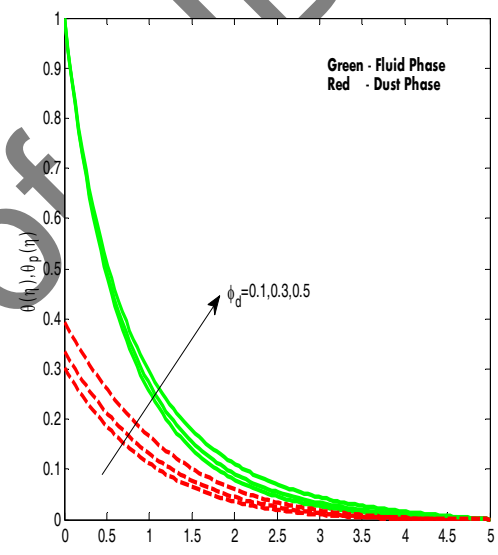


Fig. 6. Temperature profiles for various values of volume fraction of dust particles.

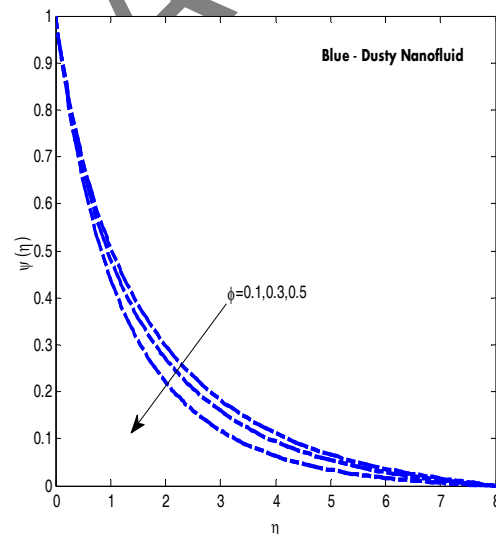


Fig. 4. Concentration profiles for various values of volume fraction of nano particles.

Figures. 5-7 illustrate the effect of volume fraction of dust particles on the velocity, temperature and concentration profiles of the flow. A raise in the volume fraction of dust particles causes to increase the velocity, temperature profiles of the fluid and dust phases and reduce the concentration profiles of the flow. But we identified a significant variation in the development of velocity and temperature profiles of the dust phase near the wall. In Figures.1and 2 the velocity and temperature profiles of the dust phase attains its maximum value near the plate. But in Figs. 5 and 6 we observed the maximum value attained by the velocity and temperature profiles are less when compared with the volume fraction of dust particles case. It is also observed in Fig.2 that the velocity profiles reaches to the free stream velocity at $\eta_{\infty} = 3$ level. But in Fig.4 the velocity profiles reached to the free stream velocity at $\eta_{\infty} = 2.5$. This concludes that an increase

in the volume fraction of nano particles effectively enhances the momentum and thermal boundary layer thickness compared with the increase in the volume fraction of dust particles.

reduces the velocity boundary layer and enhances the thermal boundary layer. Due to the variation in buoyancy forces we noticed the enhancement in the concentration profiles flow.

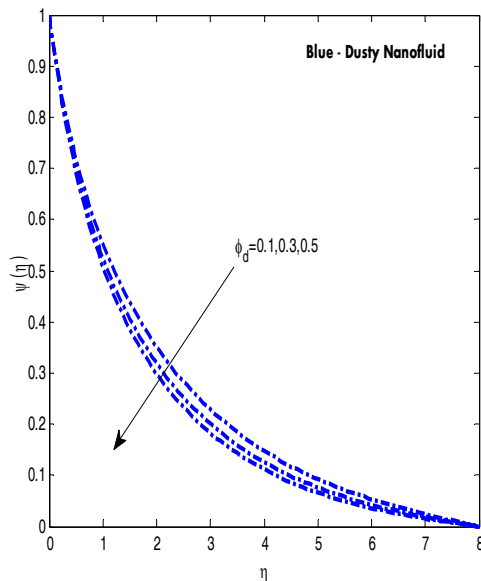


Fig. 7. Concentration profiles for various values of volume fraction of dust particles.

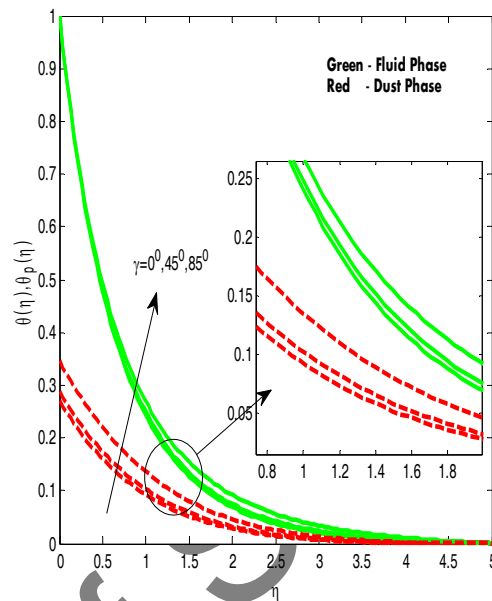


Fig. 9. Temperature profiles for various values of inclined angle.

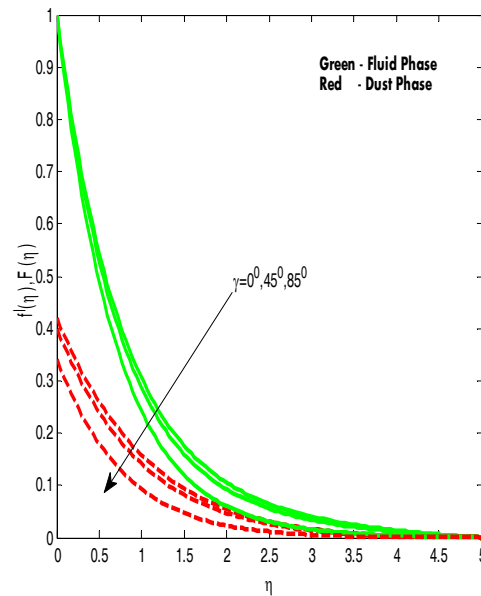


Fig. 8. Velocity profiles for various values of inclined angle.

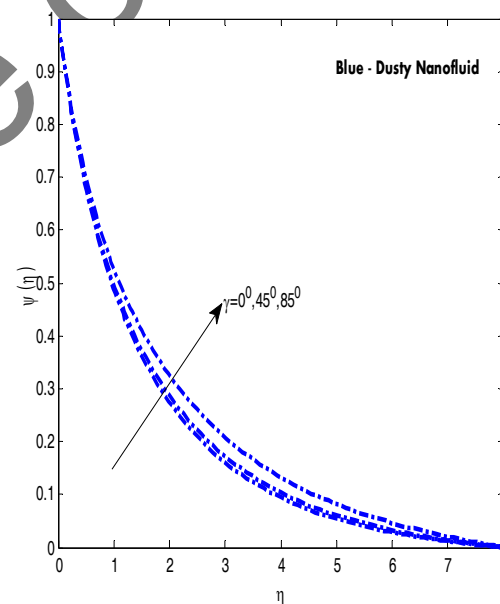


Fig. 10. Concentration profiles for various values of inclined angle.

Figures. 8-10 display the influence of inclined angle on the velocity, temperature and concentration profiles of the flow. We have noticed an interesting result that an increase in the inclined angle depreciates the velocity field and increases the temperature and concentration fields. This is due to the fact that at $\gamma = 0$ the sheet is in vertical direction and maximum gravitational force acts on the flow. As $\gamma \rightarrow \pi/2$ the sheet takes horizontal direction, the strength of buoyancy forces decreases and hence

Figure.11 represents the effect of radiation parameter on the temperature profiles of the flow. It is clear that a raise in the value of radiation parameter enhances the temperature profiles of the fluid and particle phase. Generally, an increase in the radiation parameter releases the heat energy to the flow. This causes to increase the thermal boundary layer thickness. In view of this we can conclude that influence of radiation is more

significant if $R \neq 0$ and it can be neglected as $R \rightarrow \infty$. This agrees the general physical behaviour of the radiation parameter. The effect of mass concentration of the dust particles on the temperature profiles of the fluid and dust phases are displayed in Fig.12. It is observed that a raise in the mass concentration of the dust particles depreciates the temperature fields of fluid and dust phases.

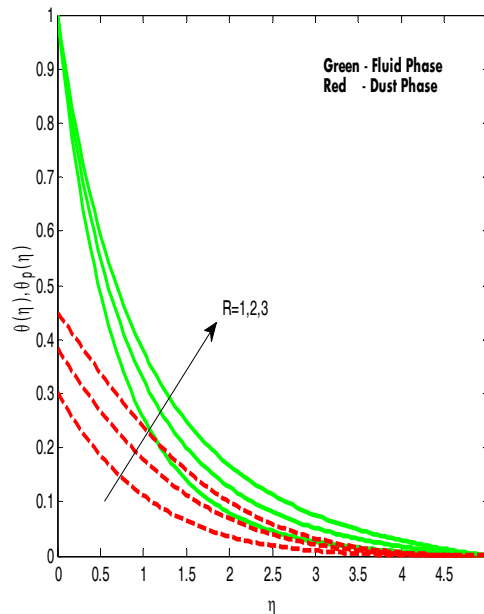


Fig. 11. Temperature profiles for various values of radiation parameter.

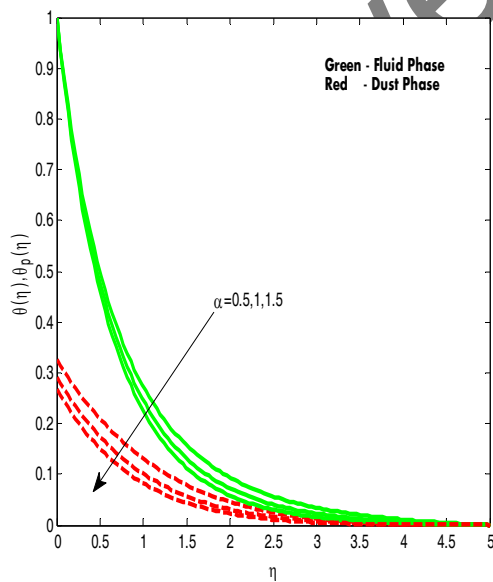


Fig. 12. Temperature profiles for various values of mass concentration of dust particles.

Figure 13 illustrates the influence of fluid particle interaction parameter for temperature (β_T) on temperature profiles of the fluid and dust phases. We observed an interesting result that an increase in the value of β_T enhances the temperature profiles

of the dust phase and depreciates the temperature profiles of the fluid phase. This is due to the fact that a raise in the fluid particle interaction parameter increases the thermal conductivity of the flow. Due to this reason we noticed depreciation in the temperature profiles of the fluid phase and increase in the heat transfer rate. The influence of chemical reaction parameter on the concentration profiles of the flow is depicted in Fig. 14. It is clear that an increase in the chemical reaction parameter depreciates the concentration profiles and increases the mass transfer rate of the dusty nanofluid.

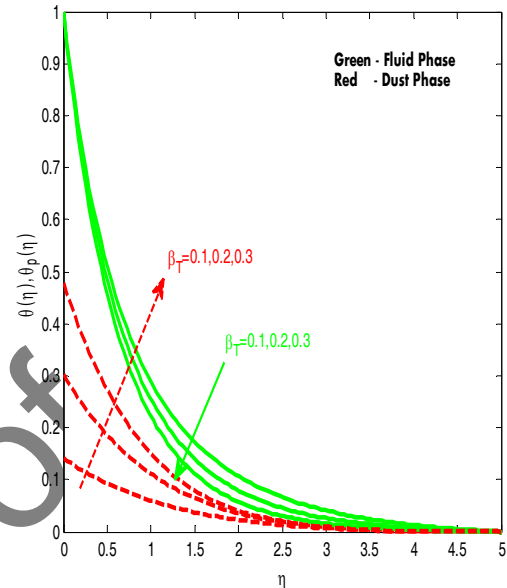


Fig. 13. Temperature profiles for various values of fluid particle interaction parameter.

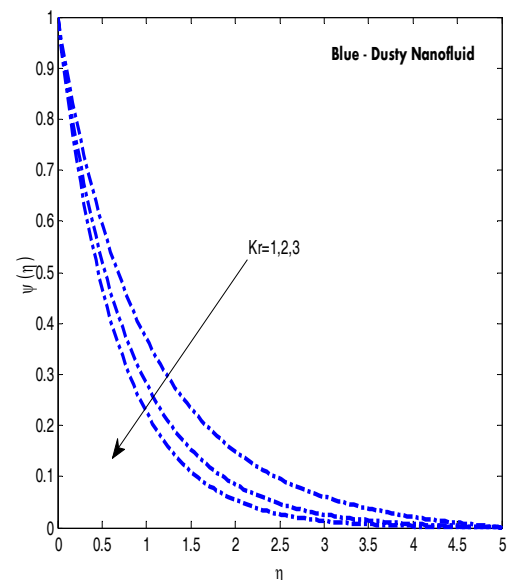


Fig. 14. Concentration profiles for various values of chemical reaction parameter.

Figures 15 and 16 present the effect of non-uniform heat source/sink parameters on the temperature profiles of the fluid and dust phases. It is observed

that a raise in the values of A^* and B^* enhances the temperature profiles of the fluid and dust phases. It is evident to conclude that the positive values of A^* and B^* acts like heat generators and negative values are acts like heat observers. Generally generating the heat releases the heat energy to the flow. This causes to enhance the temperature profiles of the flow. Hence A^* and B^* obeys the general physical property of heat source parameter.

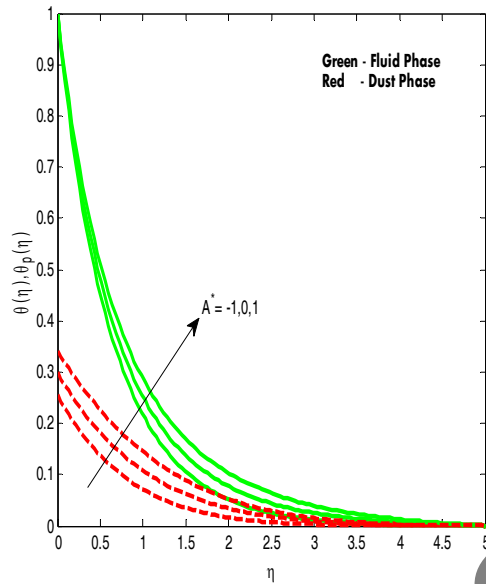


Fig. 15. Temperature profiles for various values of non-uniform heat source/sink.

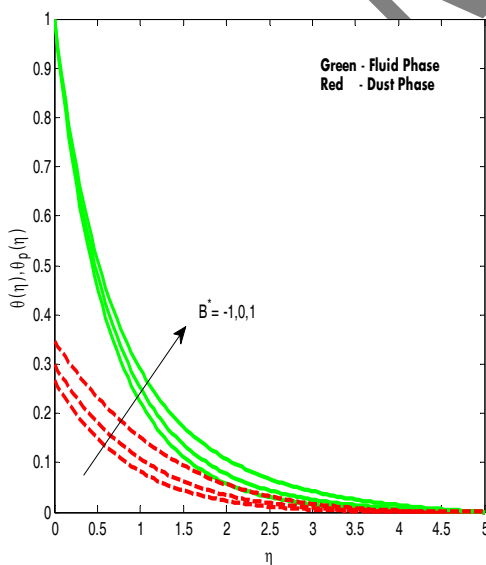


Fig. 16. Temperature profiles for various values of non-uniform heat source/sink.

Table 2 shows the comparisons of the present results with the existed results of Ramesh *et al.* (2012). Under some special conditions present

results have an excellent agreement with the existed results. This shows the validity of the present results along with the numerical technique we used in this study. Table 3 depicts the influence of non-dimensional governing parameters on friction factor, Nusselt and Sherwood numbers. It is evident from the table that a raise in the values of inclined angle and volume fraction of dust particles depreciates the skin friction coefficient, heat and mass transfer rate. Generally, an increase in the inclination causes to reduce the buoyancy forces acts on the flow. This help to decrease the friction factor along with heat and mass transfer rate. An increase in the mass concentration of dust particles and fluid particle interaction parameter for temperature declines the friction factor, Sherwood number and enhances the heat transfer rate. This is due to an increasing thermal conductivity of the flow. An enhancement in the values of radiation parameter, non-uniform heat source/sink parameter and chemical reaction parameter increases the coefficient of skin friction, mass transfer rate and reduces the Nusselt number. Physically, generating the external heat develops the friction near the wall. Due to this reason we have seen a raise in the friction factor. A raise in the value of volume fraction of nano particle depreciates the friction factor and enhances the heat and mass transfer rate. Increasing values of nano particles volume fraction enhances the interaction between the fluid and particle phase, this leads to increase the heat and mass transfer rate.

5. CONCLUSIONS

This paper presents a numerical solution for momentum, heat and mass transfer behaviour of MHD nanofluid embedded with the conducting dust particles past an inclined permeable stretching sheet. The conclusions are as follows:

- An increase in the volume fraction of nano particles enhances the heat and mass transfer rate of the dusty nanofluid.
- A raise in the values of volume fraction of dust particles enhances the thermal conductivity of the dusty nanofluid.
- An enhancement in the inclined angle depreciates the friction factor, Nusselt and Sherwood numbers.
- An increase in the mass concentration of the dust particles enhances the heat transfer rate.
- Chemical reaction parameter have tendency to reduce the concentration profiles and enhance the mass transfer rate of the dusty nanofluid.
- Reduction in wall friction helpful in cooling management in oil recovery management.
- Reduction in temperature profiles and increase in heat transfer rate is most useful in production industries.
- In non-uniform heat source/sink positive parameters acts like heat generators while negative parameters are acts like heat absorbers.

Table 2 Comparison of the values of $-\theta'(0)$ when $\phi = \phi_d = Gc = Sc = Kr = R = 0$

β	Ec	Pr	G	γ	A^*	M	Ramesh <i>et al.</i> (2012)	Present Study
0.5	0	1	.5	30^0	.5	3	0.71588	0.7158812
	1						0.51878	0.5187823
	2						0.32170	0.3217032
0.5	2	1	.5	0^0	.5	3	1.01930	1.0193012
				30^0			0.98397	0.9839713
				90^0			0.94359	0.9435901
0.5	2	1	.5	30^0	.5	1	0.53643	0.5364312
						2	0.44219	0.4421923
						3	0.32170	0.3217013

Table 3 Variation in friction factor, Nusselt and Sherwood numbers for Cu-water dusty nanofluid

γ	ϕ	ϕ_d	R	α	β_T	A^*	Kr	$f''(0)$	$-\theta'(0)$	$-\psi'(0)$
0^0								-1.596186	2.087094	0.852617
45^0								-1.677734	2.073174	0.839850
85^0								-1.859326	2.043395	0.807869
	0.1							-1.736303	2.063273	0.830135
	0.3							-2.819446	2.885399	0.862398
	0.5							-5.139467	3.866280	0.914102
		0.1						-1.736303	2.063273	0.830135
		0.3						-1.911345	2.033624	0.806536
		0.5						-2.199456	1.986362	0.770331
			1					-1.736303	2.063273	0.830135
			2					-1.730995	1.720366	0.832100
			3					-1.727216	1.501723	0.833618
				0.5				-1.735135	2.007315	0.830642
				1.0				-1.736981	2.097939	0.829855
				1.5				-1.738435	2.178052	0.829288
					0.1			-1.734030	1.948728	0.831103
					0.2			-1.736303	2.063273	0.830135
					0.3			-1.738638	2.196274	0.829238
						1		-1.739074	2.218119	0.829030
						2		-1.736556	2.077365	0.830034
						3		-1.734022	1.936312	0.831045
							1	-1.745034	2.062587	1.094642
							2	-1.751259	2.061590	1.340378
							3	-1.755486	2.060714	1.543284

REFERENCES

- Afify, A. A. (2009). Similarity solution in MHD effects of thermal diffusion and diffusion thermo on free convective heat and mass transfer over a stretching surface considering suction or injection. *Commun Nonlinear Sci Numer Simulation* 14(5), 2202-2214.
- Buongiorno, J. (2005). Convective transport in nanofluids. *Journal of Heat Transfer* 128(3), 240-250.
- Chamkha, A. J. (1998) Unsteady hydromagnetic flow and heat transfer from a non-isothermal stretching sheet immersed in a porous medium. *International Communications in Heat and Mass Transfer* 25(6), 899-906.
- Choi, S. U. S. (1995). Enhancing thermal conductivity of fluids with nanoparticles. *The Proceedings of the 1995 ASME International Mechanical Engineering Congress and Exposition*, San Francisco, USA, ASME, FED 231/MD, 99-105.
- Choudhury, R. and S. Kumar Das (2014). Visco-elastic MHD free convective flow through porous media in presence of radiation and chemical reaction with heat and mass transfer.
- Debnath, L. and A. K. Ghosh (1988). On unsteady hydromagnetic flows of a dusty fluid between two oscillating plates. *Appl. Scientific Res.* 45(4), 353-365.
- Elbashbeshy, E. M. A. (2001). Heat Transfer over an exponentially stretching continuous surface with suction. *Archives of Mechanics* 53(6), 643-651.
- Ferdows, M. S., S. M. Chapal and A. A. Afify (2014). Boundary layer flow and heat transfer of a nanofluid over a permeable unsteady stretching sheet with viscous dissipation. *J. Eng. Thermophysics* 23(3), 216-228.
- Gireesha, B. J., G. S. Roopa, H. J. Lokesh and C. S. Bagewadi (2012). MHD flow and heat transfer of a dusty fluid over a stretching sheet. *Int. J. physical and mathematical sciences.* 3(1), 171-180.
- Hassan, H. (2014). Heat transfer of Cu-water nanofluid in an enclosure with a heat sink and discrete heat source. *European J. Mechanics B/Fluids* 45, 72-83.
- Hina, S., M. Mustafa, T. Hayat and N. D. Alotaibi (2015). On peristaltic motion of pseudo plastic fluid in a curved channel with heat or mass transfer and wall properties. *Applied Math. Computation* 263, 378-391.
- Ibrahim Saidu, W., M. M. Abubakar Roko and H. Musa (2010). MHD effects on convective flow of dusty viscous fluid with volume fraction of dust particles. *ARPJ J of Eng and applied sciences.* 5, 86-91.
- Ishak, A., R. Nazar and I. Pop (2009). The effects of transpiration on the flow and heat transfer over a moving permeable surface in a parallel stream. *Che. Eng. J.* 148(1), 63-67.
- Kabir, M. A. and M. A. L. Mahbub (2012). Effects of Thermophoresis on Unsteady MHD Free Convective Heat and Mass Transfer along an inclined Porous Plate with Heat Generation in Presence of Magnetic Field. *Open Journal of Fluid Dynamics* 2, 120-129.
- Kierkus W. T. (1968) An analysis of Laminar free convection flow and heat transfer about an inclined isothermal plate. *Int. J. Heat and Mass transfer.* 11(2), 241-253.
- Krishnamurthy, M. R., B. C. Prasannakumara and B. J. Gireesha (2015). Effect of viscous dissipation on hydromagnetic fluid flow and heat transfer of nanofluid over an exponentially stretching sheet with fluid particle suspension. *Cogent Mathematics*, 2(1), ID 1050973.
- Krishnamurthy, M. R., B. C. Prasannakumara, B. J. Gireesha and G. Rama Subba Reddy (2015). Effect of chemical reaction on MHD boundary layer flow and melting heat transfer of Williamson nanofluid in porous medium. *Eng. Sci and Tech an Int. J.* 18(4), 1-8.
- Makinde, O. D. and A. Aziz (2011). Boundary layer flow of a nanofluid past a stretching sheet with convective boundary condition. *Int. J. Ther. Sci.* 50(7), 1326-1332.
- Makinde, O. D. (2005). Free convection flow with thermal radiation and mass transfer past a moving vertical porous plate. *Int. Commun. Heat Mass Transfer* 32(10), 1411-1419.
- Malyand, A., F. Hedayati and D. D. Ganji (2014). Slip effects on unsteady stagnation point flow of Nanofluid over a stretching sheet. *J Power Technology* 253, 377-384.
- Mansour, M. A., N. F. E. Anssary and A. M Aly (2008) Effects of chemical reaction and thermal stratification on MHD free convective heat and mass transfer over a vertical stretching surface embedded in a porous media considering Soret and Dufour numbers. *Chemical eng. J* 145(2), 340-345.
- Mohankrishna, P., V. Sugunamma and N. Sandeep (2014). Radiation and magnetic field effects on unsteady natural convection flow of a nanofluid past an infinite vertical plate with heat source. *Chemical and Process Engineering Research* 25, 39-52.
- Palani, G. and P. Ganesan (2007). Heat transfer effects on dusty gas flow past a semi-infinite inclined plate. *Forschung Ingenieurwesen*, 71(3-4), 223-230.
- Prasad, K.V., K. Vajravelu and P. S. Datti (2010). The effects of variable fluid properties on the hydro-magnetic flow and heat transfer over a non-linearly stretching sheet. *Int. J. of Thermal Sciences.* 49(3), 603-610.

- Ramesh, G. K., B. J. Gireesha and C. S. Bagewadi (2012). Heat transfer in MHD dusty boundary layer flow over an inclined stretching sheet with non-uniform heat source/sink. *Adv. In Mathematical Physics*, ID 657805.
- Rohni, A. M., S.Ahmad and I.Pop (2014). Flow and heat transfer at a stagnation point over an exponentially shrinking vertical sheet with suction. *Int J Thermal Sciences* 75, 164-170.
- Saffman, P. G. (1962). On the stability of laminar flow of a dusty gas. *J. Fluid Mechanics* 13(1), 120-128.
- Sandeep, N. and C. Sulochana (2015). Dual solutions for unsteady mixed convection flow of MHD Micropolar fluid over a stretching/shrinking sheet with non-uniform heat source/sink. *Eng. Science and Technology, an Int. J.* 18, 1-8.
- Sandeep, N. and V. Sugunamma (2014). Radiation and inclined magnetic field effects on unsteady MHD convective flow past an impulsively moving vertical plate in a porous medium. *Journal of Applied Fluid Mechanics* 7(2), 275-286.
- Sheikholeslami, M., D. D. Ganji, M. YounusJaved and R. Ellahi (2015). Effect of thermal radiation on magnetohydrodynamic Nanofluid flow and heat transfer by means of two phase model. *Journal of Magnetism and Magnetic Materials* 374, 36-43.
- Singh, A. K. and N.P.Singh (1996). MHD flow of a dusty visco-elastic liquid through a porous medium between two inclined parallel plates. *Proceeding of national academy of science India* 29(2), 143-150.
- Subhashini, S. V., R. Sumathi and E. Momoniat (2014). Dual solutions of a mixed convection flow near the stagnation point region over an exponentially stretching/shrinking sheet in nanofluids. *Meccanica* 49(10), 2467-2478.
- Vajravelu, K., K. V. Prasad, J. Lee, C. Lee, I. Pop and R. A. V. Gorder (2011). Convective heat transfer in the flow of viscous Ag-water and Cu-water nanofluids over a stretching surface. *Int.J.Thermal Sciences*, 50(5), 843-851.

Archive of SID

SID



سرویس های ویژه



سرویس ترجمه تخصصی



کارگاه های آموزشی



بلاگ مرکز اطلاعات علمی



عضویت در خبرنامه



فیلم های آموزشی

کارگاه های آموزشی مرکز اطلاعات علمی جهاد دانشگاهی



PROPOSAL
پروپوزال

پروپوزال نویسی و پایان نامه نویسی

دوره آموزشی

کارگاه آنلاین
پروپوزال نویسی و پایان نامه نویسی



روش تحقیق و مقاله نویسی علوم انسانی

دوره آموزشی

کارگاه آنلاین
روش تحقیق و مقاله نویسی علوم انسانی



ISI
Scopus

آشنایی با پایگاه های اطلاعات علمی بین المللی و ترند های جستجو

دوره آموزشی

کارگاه آنلاین آشنایی با پایگاه های اطلاعات علمی بین المللی و ترند های جستجو